LD pumped cryogenic-cooled Yb:YAG disk regenerative amplifier

Wenfa Huang (黄文发), Jiangfeng Wang (王江峰), Xinghua Lu (卢兴华), and Xuechun Li (李学春)*

Shanghai Institute of Optics and Fine Mechanics, Chinese Academy of Sciences, Shanghai 201800, China

**Corresponding author: lixuechun@siom.ac.cn*

Received May 24, 2012; accepted June 25, 2012; posted online November 27, 2012

A diode-pumped cryogenic-cooled Yb:YAG regenerative amplifier based on the thin disk concept, producing 14.2-mJ, 10-ns pulses with optical-to-optical conversion efficiency of ∼7% at a repetition rate of 10 Hz at 163 K, is presented.

OCIS codes: 140.3280, 140.3480, 140.3615, 140.4480.
doi: 10.3788/COL201210.S21412.

With the improvement of the high power laser diodes, ytterbium (Yb^{3+})-doped gain materials have recently attracted a great deal of interest as a laser material for a diode-pumped high-power laser with high efficiency and compact structure[1,2]. Ytterbium ion (Yb^{3+}) presents appealing properties[3−5]. Its simple electronic scheme made of only two electronic levels spitted in sublevels by the Stark effect, avoiding the excited state absorption, up conversion processes, and concentration quenching. Among various kinds of laser host materials, yttrium aluminum garnet (YAG) has been focused on due to its excellent thermal, chemical, and mechanical properties[6−9]. Yb:YAG has numerous advantages[10]. Firstly, it has wide absorption bandwidth which is suitable for direct diode pumping. In addition, a long fluorescence lifetime benefits energy storage and a very low quantum defect enables efficient and high repetition rate operation. Lastly, the thermal conductivity of the Yb:YAG crystal of 14 W/(m·K) is high among various ytterbium-doped laser materials, resulting in less heat generation during lasing than other host materials based laser systems. Several types of Yb:YAG lasers have been developed for efficient oscillation with various pumped architectures, including thin disk, microchip, and rod structures at room temperature[11−13]. However, higher pump intensities are required for room-temperature Yb:YAG lasers to overcome the thermal population of the lower lasing level and to reach high storage efficiency, due to the proximity of the lower lasing level to the ground-state. This makes it difficult to realize the full potential of the laser system at room-temperature. However, cryogenic cooling operation can overcome this disadvantage. The benefits of cooling Yb:YAG result in a drastically increase of the emission and absorption cross sections, leading to low saturation fluorescence that limits the extraction efficiency. Moreover, the thermal conductivity increases and both the thermal expansion and the thermal dispersion decrease, and the terminal level of the laser transition is unpopulated and the amplifier medium acts as a four-level system leading to high efficiency even at low pump power. Therefore, Yb:YAG crystal is one of the most promising laser materials for high-average-power operation[14]. As large output energy is required, large transverse sizes amplifier must be used. Then, longitudinal pumping makes possible homogeneous pump energy deposition in the amplifier. In this pumping configuration, the amplifier can be cooled by the rear face. In order to get efficient cooling, thin disk amplifier must be used. By taking these advantages of cryogenically-cooled Yb:YAG, we report that we have developed a compact diode end-pumped nanosecond Yb:YAG thin disk regenerative amplifier that use a liquid-nitrogen-cooled Yb:YAG crystal with the concentration of 10% in this letter. As a result, a high output amplified pulse energy of 14.2 mJ is achieved with a 10-ns pulse duration at 10-Hz repetition rate, the magnification exceeds 10^7 with an optical conversion efficiency of ∼7%.

A schematic diagram of the regenerative amplifier with a cooled Yb:YAG crystal is shown in Fig. 1. For seeding, the seed pulse is from a continuous wave (CW) distributed feedback fiber laser after an acoustic-optic chopper and optical fiber amplifiers, which produce 10-ns pulses with a 10-Hz repetition rate at a wavelength of about 1 030 nm. The pulse energies are about 120 pJ. The seed pulse is injected into the regenerative amplifier after matching the spatial mode of the seed beam to the eigenmode of the TEM_{00} cavity with a telescope. To protect the seed laser system from the much higher energy regenerative output leakage which naturally propagates in the reverse direction, a dual stage optical isolator (consists of a thin film polarizer, a Faraday rotator and a half wave plate) is used. The laser cavity of the amplifier resonator is a folded, linear one with a whole cavity length of 3 m, consists of 2 flat concave mirrors. A convex lens with a focal length of $f = 3.5$ m is placed inside the cavity to make a stable cavity resonator and compensate the thermal lensing effect either. The KD*P-Pockels cell, $\lambda/4$ plate and a thin film polarizer are used for seed pulse trapping and amplified pulse dumping. Once the seed pulse passes through the Pockels cell, the quarter-wave voltage is applied to the Pockels cell, and the pulse is trapped in the resonator for approximately 20 round trips and amplified in the cooled Yb:YAG crystal until the Pockels cell voltage is switched off again. A 400-μm-core fiber-coupled laser diode is used as a quasi CW pump source and strongly focused onto Yb:YAG crystal through the lenses. The central wavelength of the diode emission is 937.5 nm. The pump duration is 1.8 ms, and the repetition rate is 10 Hz with a maximum

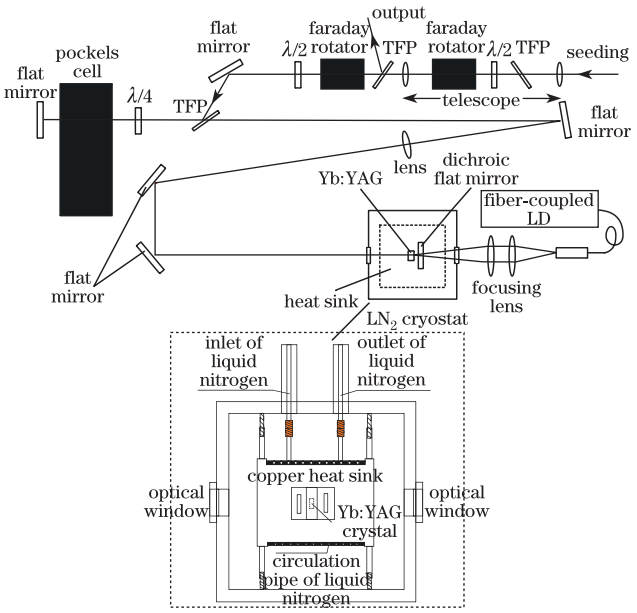

Fig. 1. Experimental setup of cryogenically-cooled Yb:YAG regenerative amplifier.

pump power of 120 W. The pump beam was focused into the laser crystal through the dichroic flat mirror. The spatial profile of the pump beam on the laser crystal had a nearly Gaussian profile with $\phi 2$ mm, which resulted in the maximum pump intensity of 6.37 kW/cm^2. The laser material was a 10-at.-% doped Yb:YAG crystal with a size of $\phi 10 \times 3$ mm. One end face of the crystal is coated for high transmission at the pump and lasing wavelengths and directly contact to the indium foil, while the opposite end face had an antireflection coating for pump wavelength. In previous work[15], Yb:YAG crystal was used as the active end mirror. The laser material is mounted on a copper holder attached to liquid nitrogen cryostat in vacuum as shown in the inset of Fig. 1. The crystal is uniformly cooled through the transverse surface, which is in contact with the heat sinks cooled by liquid nitrogen to remove the heat generated in the crystal. This open cycle cooling approach vents gas to the atmosphere after the cryogen passes through the heat sinks, removing heat from the crystal. An indium foil placed between the crystal side faces and the heat sinks provides efficient thermal contact. A temperature monitoring unit is buried in the holder near the crystal, the stability of temperature controlled by the heater is ± 0.2 K at the maximum pump power.

Fluorescence spectra of Yb:YAG is measured in order to determine stimulated emission cross section. Representative emission spectra of 10-at.-% Yb:YAG at low temperature are shown in Fig. 2. The emission strength is greater and the line shape of the emission line shape becomes narrower (from 1.3 to 0.7 nm) as the temperature decreases. The ytterbium emission from YAG is not polarization dependent, so we can use the emission spectra obtained to calculate the effective stimulated emission cross section of an Yb^{3+} ion from the manifold ${}^2F_{5/2} \rightarrow {}^2F_{7/2}$ transitions in Yb:YAG by applying the F-L formula[16]. The fundamental relationship between spontaneous-emission distribution $E(\lambda) = I(\lambda)/\int I(\lambda)\mathrm{d}\lambda$ (integrating over all ${}^2F_{5/2} \rightarrow {}^2F_{7/2}$ transitions) and stimulated emission cross section distribution $\sigma_{\mathrm{em}}(\lambda)$ is

$$\sigma_{\mathrm{em}}(\lambda) = \frac{\lambda^5}{8\pi n^2 c\tau} \frac{I(\lambda)}{\int I(\lambda)\lambda \mathrm{d}\lambda}, \quad (1)$$

where τ is the radiative lifetime of the upper laser level, c is the velocity of light in vacuum, and n is the refractive index at the emission wavelength (at 1 030 nm, n is 1.82), and $I(\lambda)$ is the emission spectral intensity of emission of the Yb^{3+} ions. The calculated emission cross section for Yb:YAG crystal at the regenerative amplifier operation temperature of 163 K is approximately 6.2×10^{-20} cm^2.

Figure 3 shows output amplified pulse energy as a function of diode pumping power at a repetition rate of 10 Hz. The output pulse energy of the regenerative amplifier increases with increasing peak power of the pump beam. An output pulse energy of 14.2 mJ is obtained with about 20 round trips at an pump power of 115 W with the optical-optical efficiency of ~7%. Higher efficiency will be obtained at lower temperature and higher pump power. However, more pump power is not supplied in order to avoid optical damage. The beam spatial profile is measured as shown in the inset of Fig. 3. A slight ellipticity of the output pulse may be caused by the thermal effects.

In conclusion, we develope a compact diode back end-pumped regenerative amplifier with a cryogenic-cooled Yb:YAG crystal. At 115 W of the input pump power, the output pulses energy from the regenerative

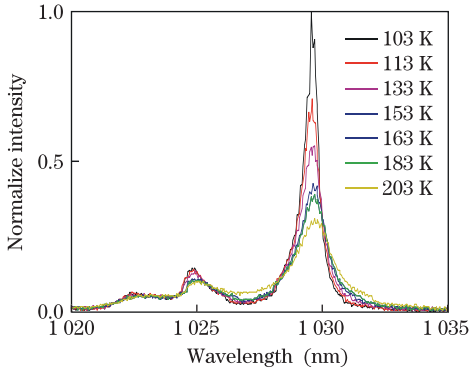

Fig. 2. Emission spectra for Yb:YAG.

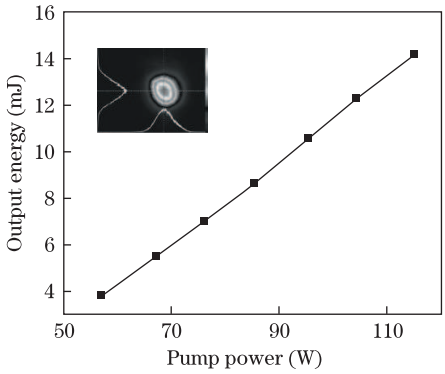

Fig. 3. Output characteristic of cryogenically-cooled Yb:YAG regenerative amplifier as a function of input LD peak power. The subfigure shows the spatial beam profile of the amplified pulse.

amplifier at 1 030 nm is 14.2 mJ at 163 K. The magnification exceeds 10^7 with the optical to optical conversion efficiency of ∼7%. Such a multi-mJ, multi-Hz range Yb:YAG regenerative amplifier provides a new concept for high-pulse-energy operation with high repetition rate in the inertial fusion energy (IFE) driver and is useful for an optical parametric chirped pulse amplification pump source.

References

1. A. H. Curtis, B. A. Reagan, K. A. Wernsing, F. J. Furch, B. M. Luther, and J. J. Rocca, Opt. Lett. **36,** 2164 (2011).
2. P. Russbueldt, T. Mans, J. Weitenberg, H. D. Hoffmann, and R. Poprawe, Opt. Lett. **35,** 4169 (2011).
3. G. L. Bourdet, Opt. Commun. **200,** 331(2001).
4. C. D. Marshall, S. A. Payne, L. K. Smith, H. T. Powell, W. F. Krupke, and B. H. T. Chai, IEEE J. Selected Topics in Quantum Electronics **1,** 67 (1995).
5. J. Lu, K. Takaichi, T. Uematsu, A. Shirakawa, M. Musha, J. F. Bisson, K. Ueda, H. Yagi, T. Yanagitani, and A. A. Kaminskii, Laser Physics **13,** 940 (2003).
6. P. H. Klein and W. J. Croft, J. Appl. Phys. **38,** 1603 (1967).
7. G. A. Slack and D. W. Oliver, Phys. Rev. B **4,** 592 (1971).
8. T. Fan and J. Daneu, Appl. Opt. **37,** 1635 (1998).
9. R. Wynne, J. L. Daneu, and T. Y. Fan, Appl. Opt. **38,** 3282 (1999).
10. W. Koechner, *Solid-State Laser Engineering* (Springer-Verlag, Berlin, 1999).
11. E. Innerhofer, T. Südmeyer, F. Brunner, R. Häring, A. Aschwanden, R. Paschotta, C. Hönninger, M. Kumkar, and U. Keller, Opt. Lett. **28,** 367 (2003).
12. J. Dong, A. Shirakawa, K. I. Ueda, and A. A. Kaminskii, Appl. Phys. B: Lasers and Optics **89,** 359 (2007).
13. S. Wang, J. Chen, C. Liu, M. Hu, J. Ge, G. Zhao, and J. Xu. Chinese J. Lasers (in Chinese) **36,** 23 (2009).
14. S. Tokita, J. Kawanaka, Y. Izawa, M. Fujita, and T. Kawashima, Opt. Express **15,** 3955 (2007).
15. J. F. Wang, Y. E Jiang, X. C. Li, and X. Li, Proc. SPIE **7916,** 79160M (2011).
16. J. Dong, M. Bass, Y. L. Mao, P. Z. Deng, and F. X. Gan. J. Opt. Soc. Am. B **20,** 1975 (2003).